Contrast Threshold of a Brisk-Transient Ganglion Cell In Vitro

Narender K. Dhingra, Yen-Hong Kao, Peter Sterling, and Robert G. Smith
Department of Neuroscience, University of Pennsylvania School of Medicine, Philadelphia, Pennsylvania 19104-6058

Dhingra, Narender K., Yen-Hong Kao, Peter Sterling, and Robert G. Smith. Contrast threshold of a brisk-transient ganglion cell in vitro. *J Neurophysiol* 89: 2360–2369, 2003. First published January 22, 2003; 10.1152/jn.01042.2002. We measured the contrast threshold for mammalian brisk-transient ganglion cells in vitro. Spikes were recorded extracellularly in the intact retina (guinea pig) in response to a spot with sharp onset, flashed for 100 ms over the receptive field center. Probability density functions were constructed from spike responses to stimulus contrasts that bracketed threshold. Then an "ideal observer" (IO) compared additional trials to these probability distributions and decided, using a single-interval, two-alternative forced-choice procedure, which contrasts had most likely been presented. From these decisions we constructed neurometric functions that yielded the threshold contrast by linear interpolation. Based on the number of spikes in a response, the IO detected contrasts as low as 1% [$4.2 \pm 0.4\%$ (SE); $n = 35$]; based on the temporal pattern of spikes, the IO detected contrasts as low as 0.8% ($2.8 \pm 0.2\%$). Contrast increments above a very low "basal contrast" were discriminated with greater sensitivity than they were detected against the background. Performance was optimal near 37°C and declined with a Q_{10} of about 2, similar to that of retinal metabolism. By the method used by previous in vivo studies of brisk-transient cells, our most sensitive cells had similar thresholds. The in vitro measurements thus provide an important benchmark for comparing sensitivity of neurons upstream (cone and bipolar cell) and downstream to assess efficiency of retinal and central circuits.

INTRODUCTION

The retinal ganglion cell presents a functional "bottleneck" on the visual pathway, receiving input from hundreds of photoreceptors and sending output to hundreds of cortical cells (Barlow 1981; Meister and Berry 1999). Consequently, it is a key locus to measure visual thresholds. Knowing a ganglion cell's threshold, one could compare the thresholds of neurons upstream (cone and bipolar cell) and thus determine the efficiency of retinal circuits. Similarly, one could compare thresholds of neurons downstream (geniculate and cortical cells), and even behavior, and thus assess the efficiency of central circuits. We chose to measure ganglion cell threshold in vitro because this would facilitate subsequent measurement of the upstream neurons. Furthermore, we could compare with previous studies in vivo to determine whether sensitivity is preserved when the retina is placed in vitro.

Ganglion cell thresholds have been previously measured as the stimulus magnitude that changes the maintained discharge by a criterion value (Barlow and Levick 1969; Derrington and

Lennie 1982; Enroth-Cugell and Robson 1966; Linsenmeier et al. 1982). However, this method of threshold measurement sets constant rates of false positive and false negative responses (Barlow and Levick 1969; Derrington and Lennie 1982) that may underestimate sensitivity (see DISCUSSION). Moreover, this method assesses only the spike count, whereas additional information may be present in the pattern of spike rate or in spike timing (Geisler et al. 1991; Meister and Berry 1999; VanRullen and Thorpe 2002). Consequently, we chose to measure threshold using an "ideal observer" (IO) that would minimize the total errors, thus optimally estimating sensitivity, and would assess different features of the spike train (Geisler et al. 1991). Here we report contrast thresholds of brisk-transient ganglion cells in the visual streak of guinea pig retina in vitro measured under photopic backgrounds.

METHODS

Animals and tissue preparation

Retinas were obtained from adult guinea pigs (400–700 g) of either sex. An animal was anesthetized with ketamine (100 mg/kg; Abbott Laboratories, North Chicago, IL), xylazine (20 mg/kg; Phoenix Pharmaceutical, St. Joseph, MO), and pentobarbital (50 mg/kg; Abbott Laboratories). Each eye was enucleated in dim red light and hemisected at ora serrata, and the posterior eyecup was placed in oxygenated (95% O_2-5% CO_2) Ames medium (Sigma, St. Louis, MO) containing sodium bicarbonate (1.9 g/l) and glucose (0.8 g/l). The animal was killed with an overdose of pentobarbital. The retina, still attached to pigment epithelium, choroid, and sclera, was incised radially at several places and flattened with ganglion cells up on a membrane filter (type HA; Millipore, Bedford, MA). The preparation rested in the medium for approximately 30 min before recording commenced. Typically experiments were run for several (6–8) hours with robust responses to light.

Recording and stimulation

The retina was mounted in a chamber on the stage of an upright microscope (Olympus America, Melville, NY) and superfused with oxygenated Ames medium at 3–4 ml/min. The medium was warmed just before it entered the chamber, and temperature was continuously monitored near the retina with a thermocouple probe (Omega Engineering, Stamford, CT). Experiments were conducted at 35–37°C except where noted otherwise. A ganglion cell soma was visualized using infrared differential interference contrast (DIC) optics through a hole in the membrane filter and cleared of Muller cell end-feet by squirting Ames medium from a pipette (tip resistance of 3–7 MΩ) under mild pressure (Roska and Werblin 2001). A patch pipette was

then attached loosely (5–20 MΩ) by mild suction. Spikes were fed to a Neurodata IR-283 amplifier (Cygnus Technologies, Delaware Water Gap, PA), high-pass filtered at 100 Hz, and recorded at 5 kHz using Axoscope software (Axon Instruments, Foster City, CA). This frequency was a compromise between higher resolution to reduce digitization noise and smaller data storage requirements and gave 5–7 recording points per spike. The amplitude of the depolarizing phase of the extracellular spikes varied 40–50%, the amplitude of the hyperpolarizing phase varied $<10\%$, and the recorded spikes had a well-defined refractory period, all consistent with a signal from a single neuron. We observed only rarely two sets of spikes (where amplitude of both depolarizing and hyperpolarizing phases differed by more than 50% with independent timing). In these cases, the data were discarded. After recording, a cell was sometimes penetrated with a sharp electrode containing 2% Neurobiotin (Vector Laboratories, Burlingame, CA) or 0.2% DiI (Molecular Probes, Eugene, OR) and stained to visualize morphology.

Visual stimuli (spots of variable size, duration, temporal frequency, and contrast) were generated with Matlab (MathWorks, Natick, MA) using extensions provided by the high-level Psychophysics Toolbox (Brainard 1997) and the low-level Video Toolbox (Pelli 1997). The stimuli were displayed on a 3.5″ color monitor of 640 × 480 pixels with the green phosphor and a vertical frame rate of 120 Hz (custom built by MicroBrightField, Colchester, VT) with a standard VGA card and a video attenuator (ISR, Syracuse, NY) to achieve 10-bit precision for contrast. The image was projected through a 4× objective focused onto the photoreceptors. The mean stimulus background, measured with a photometer (model IL1400A, International Light, Newburyport, MA) at the microscope stage, was 7,900 photons/μm^2/s [equivalent to 820 R^*/cone/integration time (50 ms)], well into the photopic range. Total area over which the stimulus could be presented on the retina was confined to a square region of 3.7 mm (430 pixels) on the side. The relationship between voltage and monitor intensity was linearized in the software with a lookup table. Contrast was defined as $(I_{max} - I_{mean})/I_{mean}$, where $I_{mean} = [d \cdot I_{max} + (1 - d) \cdot I_{min}]$, where I_{max} and I_{min} are maximum and minimum light intensities and d is the duty cycle. For equal contrast values of square and sine waves, the amplitude of the fundamental in the square wave is 1.27 times greater, but we did not include this factor in the contrast definition when comparing performance.

IO analysis

We chose the IO method to determine contrast threshold because it requires only a few assumptions about the statistical properties of the stimulus and the neural response: 1) stimulus is temporally defined; 2) response is stationary; and 3) bins are independent. Furthermore, the IO can measure thresholds for different features of the neural response, such as the number of spikes, time to nth spike, and temporal pattern. Whether or not the brain uses these temporal features (VanRullen and Thorpe 2002), we wished to quantify how much information they might contain. Finally, the IO method resembles the two-alternative forced choice method used in psychophysical measurements, thus facilitating comparisons between neuron and behavior.

The IO measured the smallest change in contrast that was discriminable based on spike responses to equally probable stimulus contrasts, in a single-interval, two-alternative forced-choice procedure. First, it collected statistical knowledge about the two responses by constructing a probability density function (PDF) from multiple presentations of each contrast. The IO then compared each subsequent response to a pair of PDFs and decided which contrast had most likely been presented (Green and Swets 1974). These decisions were tallied and threshold taken as the contrast that gave a criterion level of correct decisions. Our criterion was 68% correct because in this single-interval paradigm it corresponds to 75% correct that is widely used in the two-interval paradigm of psychophysics (Geisler et al. 1991).

To acquire the necessary data set we presented stimuli in blocks,

each block consisting of 20 or 40 trials of a particular contrast. Blocks of different contrasts were randomly interleaved and repeated to accumulate 200–800 responses to each contrast. Sensitivity at low contrasts was maximized by allowing 5 s between blocks and discarding the first response in each block. Since responses typically recovered from adaptation in 2–3 s, there was no apparent trend in the responses after a contrast change (data not shown). The observed recovery time was shorter than previously reported (Brown and Masland 2001; Chander and Chichilnisky 2001; Smirnakis 1997) probably because our stimuli were brief and of lower contrast (typically $<10\%$).

The IO's decision could be calculated from the likelihood ratio (Geisler et al. 1991) given by

$$L = P(N_1, \ldots, N_n|\beta)/P(N_1, \ldots, N_n|\alpha) \qquad (1)$$

where N_i is the number of spikes in the ith bin, n is the number of bins, and α and β are the two stimuli. For $L > 1$, the IO chooses stimulus β; for $L < 1$, the IO chooses stimulus α. When the choice corresponds to the stimulus actually presented, it is "correct." This decision rule does not assume normal distributions of noise and is considered nearly optimal because no other decision rule can produce better average performance (see Green and Swets 1974). *Equation 1* includes all possible information in a spike train and can be implemented with a multidimensional histogram. However, this would require an impractically large amount of data. Therefore following Geisler et al. (1991), we approximated the IO with unidimensional histograms based on specific features of the spike train: spike count, time-to-spike, and temporal pattern. For spike count, *Eq. 1* was modified to (Geisler et al. 1991)

$$L = P(N|\beta)/P(N|\alpha) \qquad (2)$$

where N is the number of spikes in the entire trial period (the time from one stimulus onset to the next).

For time-to-spike, the time from stimulus onset to a spike was used to construct the probability distribution, and *Eq. 1* was modified to

$$L = \prod_{i=1}^{m} P_i(T_i|\beta)/\prod_{i=1}^{m} P_i(T_i|\alpha) \qquad (3)$$

where T_i is the time from stimulus onset to ith spike and m is the number of spikes in a trial. The time-to-spike feature assumed no uncertainty in the time of stimulus onset. Time-to-first-spike was also termed latency.

For temporal pattern, the spike response was binned in time, and a spike count distribution was constructed for each bin. In this case, *Eq. 1* was modified to

$$L = \prod_{i=1}^{n} P_i(N_i|\beta)/\prod_{i=1}^{n} P_i(N_i|\alpha) \qquad (4)$$

where N_i is the number of spikes in ith bin, and n is the number of temporal bins. Thus spike count was a form of temporal pattern with only one temporal bin.

Equations 3 and *4* assume that the bins are independent. In fact, autocorrelograms of spike trains showed that for contrasts $\leq 10\%$ correlations were present but extended for only approximately 5 ms. Because our bin size was approximately 40 ms (see RESULTS) these correlations did not significantly violate the assumption of independence.

RESULTS

This report concerns 35 ganglion cells from the visual streak (30 OFF-center, 5 ON-center). Many additional ON cells were encountered, but in our preparation, they were often difficult to

hold for long periods. These ON cells had relatively high maintained rates (20–60 Hz). The OFF cells had low maintained rates (approximately 5 Hz), probably due to the high background intensity, as previously reported (Cleland et al. 1973; Troy and Robson 1992). No differences in threshold of ON and OFF cells were apparent.

Cells were selected for the largest somas (15–25 μm diameter; Fig. 1A). Responses were uniformly "brisk-transient" (Fig. 1B) with a strong "shift-effect" (Demb et al. 1999) and prominent frequency-doubling to a fine, contrast-reversing grating (Demb et al. 2001). Stained with DiI, their monostratified, radiating dendrites covered a field 400–700 μm in diameter (Fig. 1C). When filled with neurobiotin (n = 6), they
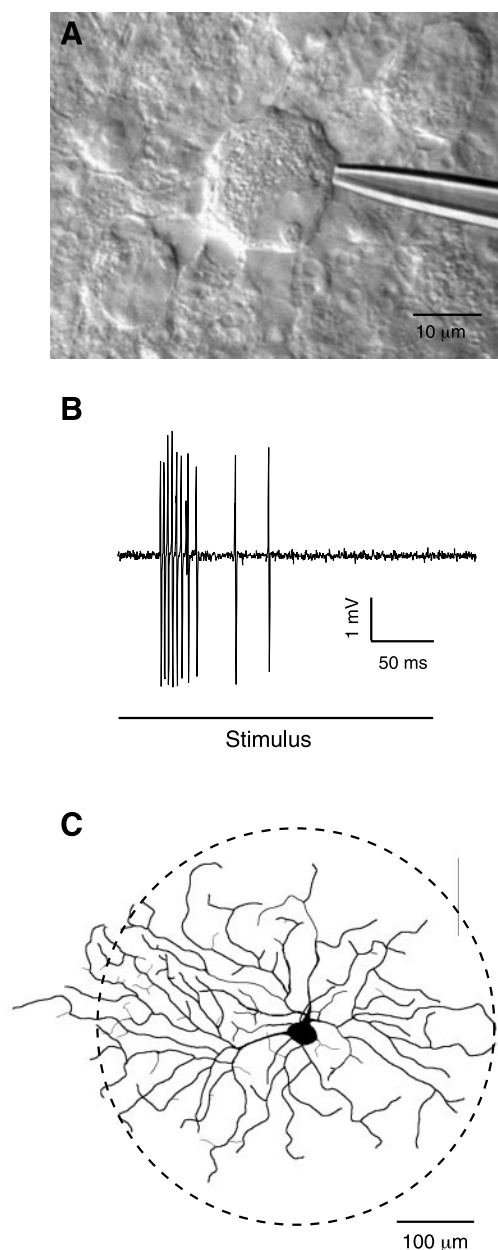

FIG. 1. OFF brisk-transient cell in vitro. A: large soma in the visual streak photographed through the differential interference contrast (DIC) optics with pipette image superimposed in loose-patch configuration. B: response to a 250-ms dark spot with 20% contrast. C: ganglion cell (same as in B) stained with DiI after the recording. Circle shows the spatial extent of the stimulus.
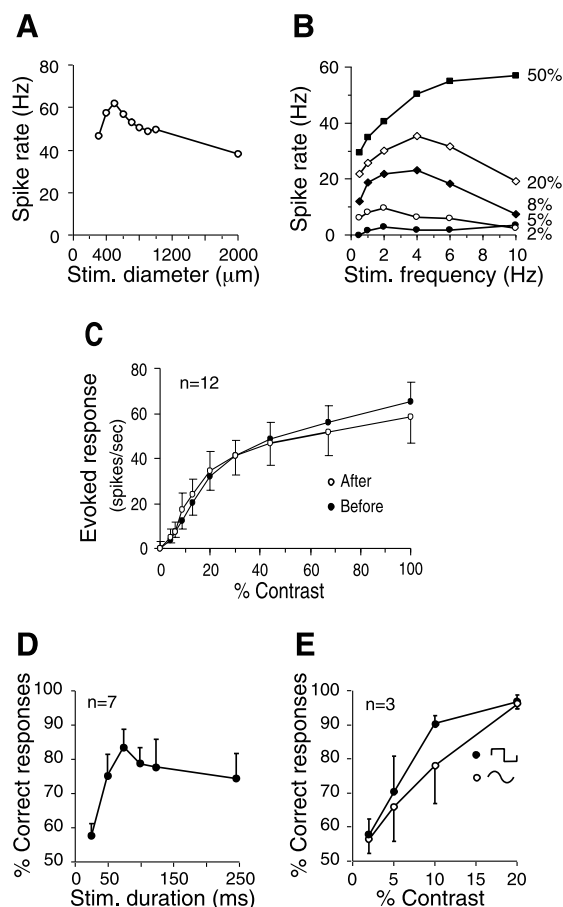

FIG. 2. Optimizing the stimulus. A: optimal diameter to 100-ms spot at 50% contrast (20 trials) was 500 μm for this cell. B: frequency response function of a cell (same as in A) at different contrasts (shown on *right*). Optimal frequency to 100-ms spot was 2 Hz at contrasts ≤5% but 4 Hz or more at higher contrasts. C: contrast response function, optimized for spot size and temporal frequency, measured before and after recording of main trials. The 2 functions are nearly identical, especially for contrasts below 50%. D: performance to an optimal spot at 5% contrast improved with stimulus duration up to 50 ms (mean ± SE). E: contrast detection was slightly better to temporal square wave than to sine wave stimuli (mean ± SE).

showed coupling to amacrine cells. Thus these cells resemble in morphology, connections, and function the "brisk-transient"/Y/α cells in cat and rabbit (Boycott and Wassle 1974; Cleland et al. 1973; DeVries and Baylor 1997; Enroth-Cugell and Robson 1966; Peichl et al. 1987; Rockhill et al. 2002).

Optimizing the stimulus

We first located the receptive field center by presenting a small spot (170 μm diameter, 50% contrast) in each square of a 5 × 5 grid centered over the cell soma. At the location with the maximum response, we enlarged the spot to find the center's extent (Fig. 2A). Optimal stimulus diameter varied from 400 to 700 μm. Then, using this spot, we tested various temporal frequencies (0.5–10 Hz sine wave) at several stimulus contrasts (2–50%). Optimal frequency increased with contrast (Fig. 2B), but we chose the one near threshold, usually 2 (n = 23) or 4 Hz (n = 12). At 2 or 4 Hz, a 100-ms square wave stimulus constituted a duty cycle of 20% or 40%. During the rest of the trial period (80% or 60%), the mean background intensity was presented. This stimulus at still lower temporal

frequencies (1–0.5 Hz) gave a slightly greater response because the inter-stimulus interval was longer, allowing more complete recovery from adaptation. However, we compromised at 2 or 4 Hz to collect an adequate number of trials at each contrast. In optimizing stimulus location, size, and frequency, we used spike rate. This was relevant to subsequent measures of performance because noise in the spike rate did not vary much with contrast (see Fig. 3F).

With the stimulus optimized, we collected the data needed to construct PDFs for the IO. This required 200–800 stimulus trials extending over 45–120 min. We checked for stationarity by measuring a contrast response function before and after the main trials and found these to be similar, especially at low contrasts (Fig. 2C). In addition, since the stimuli were presented randomly, we checked the responses to each contrast for stationarity throughout the recording session. Initial tests showed that performance improved with stimulus duration up to 50 ms [$P < 0.01$; $F(3,19) = 8.75$; one-way ANOVA; Fig. 2D]. All subsequent tests used 100 ms because this duration is commonly used in psychophysics (Banks et al. 1987; Davila and Geisler 1991). Rapid stimulus onset gave slightly better performance than graded onset (square wave vs. sine wave; Fig. 2E), presumably due to the square wave's higher contrast energy. Furthermore, the square wave stimulus with a 20% duty cycle (100 ms at 2 Hz) allowed a longer recovery time than a sine wave (50% duty cycle), increasing the independence between consecutive trials. Therefore remaining tests all used a square wave stimulus.

Optimizing the preparation: temperature

The retina's metabolic rate rises with temperature up to 37°C with a Q_{10} of 1.9 (Ames et al. 1992), and consequently one might expect neural performance to vary with temperature.

However, despite the fact that in vitro studies commonly use ambient temperature, the relationship between circuit performance and temperature has never been measured, either for retina or any other region of mammalian brain. We assessed ganglion cell performance (using temporal pattern) at four temperatures between 25°C and 37°C. Thirty-seven degrees Celsius is probably normal for the retina because guinea pig core temperature is approximately 38°C (Liu 1988), and the retina may be slightly cooler. Performance improved with temperature (Fig. 3A), reducing the contrast threshold exponentially (Fig. 3B). From 25°C to 37°C, the threshold reduced by about 2.5-fold, which extrapolates to a Q_{10} of 2.11.

Maintained firing declined with increasing temperature (Fig. 3C). However, this did not correlate with the contrast threshold and thus did not explain the lowered threshold (Fig. 3D). Such independence of threshold from maintained rate would be expected from the temporal pattern analysis because it is insensitive to changes in maintained rate (see Fig. 8B). We considered whether the improved sensitivity was mediated by increased signal, decreased noise, or both. Signal was defined as the difference in firing rates between two stimulus conditions

$$\text{Signal} = \bar{x}_\alpha - \bar{x}_\beta \tag{5}$$

where $\bar{x}$ is the peak spike rate in a 5-ms bin when the stimulus is α or β. Signal increased markedly from 25°C to 32°C but no further from 32°C to 37°C (Fig. 3E). Since in a two-alternative discrimination task noise from both stimuli might limit the performance, the noise was defined as

$$\text{Noise} = \sqrt{\sigma_\alpha^2 + \sigma_\beta^2} \tag{6}$$

where σ is the SD of the peak spike rate in a 5-ms bin when the stimulus is α or β. Noise increased modestly from 25°C to
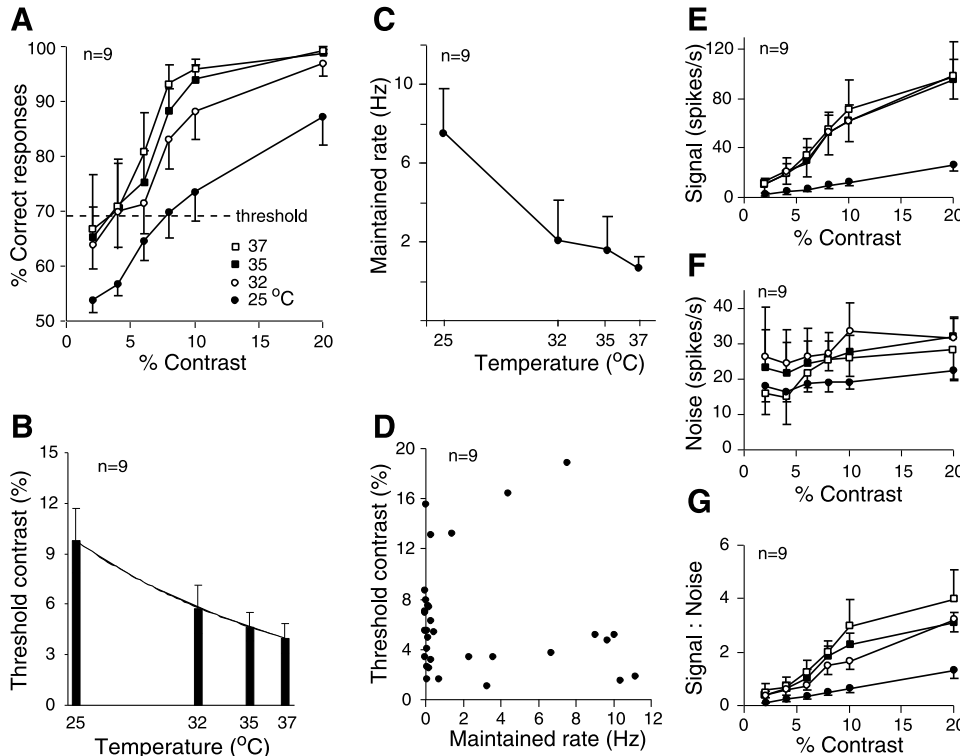

FIG. 3. Effects of temperature. A: performance increased from 25°C to 37°C (mean ± SE). Symbols also apply to E–G. B: contrast threshold declined from 25°C to 37°C (mean ± SE). Solid curve is exponential fit to the data ($Q_{10} = 2.11$). C: maintained spike rate declined with temperature (mean ± SE). D: threshold (measured with temporal pattern) did not correlate with maintained rate. Each data point represents maintained rate of 1 cell at 1 temperature. E: signal (peak rate − maintained rate) increased from 25°C to 32°C. F: noise (square root of sum of variances) declined slightly from 32°C to 37°C. G: signal to noise ratio improved systematically with temperature.

32°C but declined slightly from 32°C to 37°C (Fig. 3*F*). In short, the monotonic improvement of signal-to-noise ratio between 25°C and 37°C (Fig. 3*G*) was due to effects on both signal and noise.

Optimizing the IO

The IO was susceptible to two important sources of error: number of trials and size of temporal bins. Insufficient trials degraded performance because reference trials gave noisy PDFs, and test trials were subject to response fluctuation. As we increased the number of trials from 10 to 100, performance improved markedly and then saturated (Fig. 4*A*). The present results are all based on ≥200 trials. Excessively small time bins gave noisy PDFs, whereas larger time bins smoothed the PDFs but lost the temporal pattern (Fig. 4*B*, lower curve with diamonds). With more trials (500 or 800), performance was unaffected by bin size ≤40 ms but declined sharply for larger
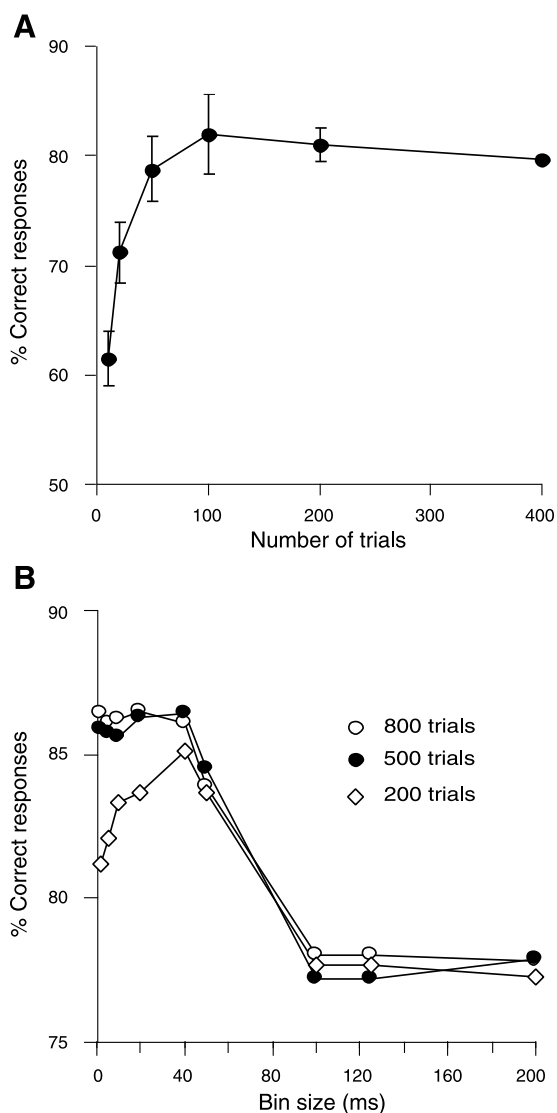
bins (Fig. 4*B*). Thus for each cell we determined an optimal bin size. This varied from 30 to 50 ms and roughly corresponded near threshold to the response duration (see Fig. 5*A*).

Contrast detection threshold

After optimizing the stimulus, the temperature, and the IO, we proceeded to measure the ganglion cell's contrast threshold. Initially we estimated threshold from the contrast response function (Fig. 2*C*). Then we presented 6–10 closely spaced contrasts to bracket the estimate and analyzed the responses with the IO. As shown in Fig. 5, the raster plots of 200 trials at each contrast allow the lowest contrast (1%) to be easily discriminated by eye from the blank trials (0%). However, a single trial with 1% or 2% contrast cannot clearly be discriminated from a blank trial (Fig. 5*A*, filled circles). Therefore to discriminate a low contrast trial from a blank requires a "best guess" based on prior information. And we wished to learn whether the best guess should be based on spike count, latency, or temporal pattern (*Eqs. 2–4*).

The "prior information" for spike count, based on 100 trials at each of two contrasts, is shown in Fig. 5*B*. Trials yielding two or three spikes are fairly likely at 2% contrast but not at 0%. Similarly, prior information for spike latency shows that a 70-ms latency is very likely at 2% contrast but not at 0% (Fig. 5*C*). Using these PDFs, the IO detected the 2% contrast with 77% correct responses for spike count and 87% correct for spike latency (Fig. 5*E*, asterisks). After similarly determining performance for additional contrasts, neurometric curves were constructed from which contrast threshold (68% correct) was determined by linear interpolation or extrapolation to 50% correct at 0% contrast (Fig. 5*E*). For this cell, the most sensitive (by pattern) that we studied, contrast threshold determined by spike count was 1.6%, whereas by spike latency it was 1% (Fig. 5*E*).

Prior information for temporal pattern is illustrated in Fig. 5*D*. The responses at each contrast were divided into temporal bins of optimal size, and the probability of $0 - n$ spikes was calculated for each bin. Temporal pattern was obtained by multiplying the PDFs of all bins to give their joint probability. Using this joint probability, the IO detected the 2% stimulus with 92% correct responses. Threshold, determined by extrapolation from the neurometric curve, was 0.8% contrast (Fig. 5*E*). This remarkably low threshold was expressed by several cells, and the average threshold was about 3% contrast (Fig. 5*F*).

Across cells, temporal pattern gave the lowest threshold: 2.8 ± 0.2%; then latency, 3.8 ± 0.5%; and count, 4.2 ± 0.4% (SE) (Fig. 6, *A* and *D*). Threshold by pattern differed significantly from latency ($P < 0.05$; $t = 1.9$; df = 68; 1-tailed *t*-test) and count ($P < 0.001$; $t = 3.4$; df = 68; 1-tailed *t*-test). Compared at contrasts above threshold, pattern again performed best. Latency performed better than count near threshold, but their curves crossed, so for contrasts >7% count performed better (Fig. 6*A*). The reason was that a stimulus near threshold evoked at most one extra spike above the maintained rate, whereas stronger stimuli evoked additional spikes (Fig. 6*B*). When time-to-spike included second and third spikes, it performed similarly to temporal pattern, improving at higher contrasts (Fig. 6*C*) but not much near threshold (Fig. 6, *C* and *D*).

FIG. 4. Optimizing the ideal observer (IO). *A*: performance at 10% contrast improved as number of trials increased from 10 to 100 (mean ± SE). Similar results were obtained for 8 cells. *B*: same cell as shown in *A*. With 200 trials, performance peaked at 40 ms. With more trials (500 or 800), performance was unaffected by bin size ≤40 but declined sharply for larger bins.
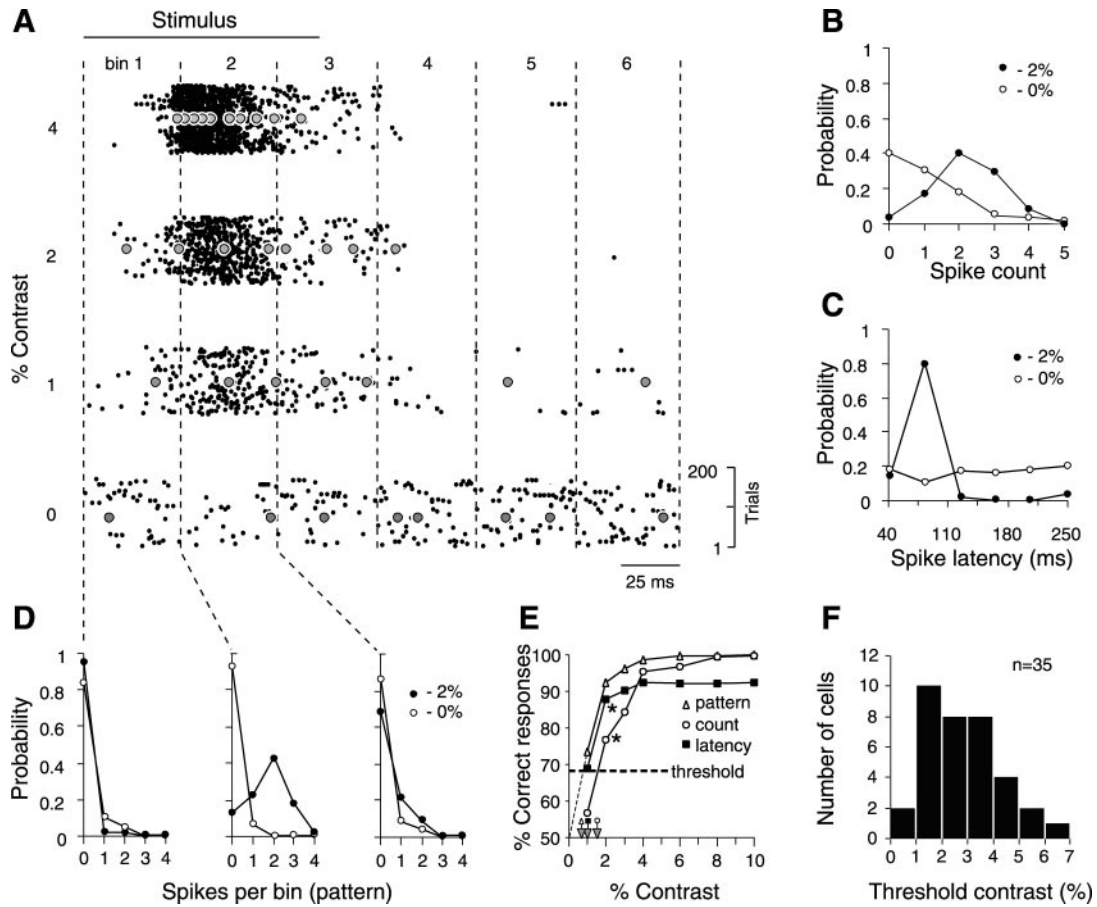
FIG. 5. IO analysis. *A*: raster plots of spike responses to 200 trials at each contrast. One-half of the trials at each contrast were selected randomly to construct probability density functions (PDFs) based on spike count (*B*), latency (*C*), and temporal pattern (*D*). Detection was measured by testing the remaining trials individually against the PDFs in a single-interval forced-choice task. Filled circles represent spike responses from randomly selected single trials at each contrast. *B*: PDFs for 0 and 2% contrasts based on spike count (spikes counted in the entire trial period from one stimulus onset to the next). *C*: spike latency: A 2% contrast was more likely than 0% to evoke the first spike at short latency. *D*: temporal pattern. Trials were divided in to multiple time bins, and PDFs were constructed for each bin. The IO used their joint probabilities for detection. *E*: neurometric curves for the 3 types of analyses. Threshold contrast (68% correct; arrows) was determined by linear interpolation (solid lines connecting data points) or by extrapolation to 50% correct at 0% contrast (dashed line). Threshold differed for each analysis. Temporal pattern gave the lowest threshold, 0.8% contrast. *F*: contrast thresholds for all cells measured with temporal pattern.

To compare our in vitro measurement with earlier in vivo measurements of the corresponding cell type in cat retina and lateral geniculate (Derrington and Lennie 1982; Troy 1983), we applied their definition of threshold (contrast required to change the maintained rate by 2 SD). By this method our most sensitive cells gave thresholds of 1% [7.2 ± 5.4 (SD); *n* = 32; Fig. 6D]. These thresholds overlap with cat brisk-transient ganglion cells, although the mean is higher (see DISCUSSION). Thresholds determined by this method were higher than those determined for the same cells by the IO method by 2.6-fold for pattern and 1.7-fold for count (Fig. 6D).

Contrast discrimination threshold

In a separate series of experiments, we tested a ganglion cell's threshold for discriminating between two fine contrasts. A center spot of optimal diameter and temporal frequency was presented for 100 ms in randomized blocks for several contrasts (0–50%), and responses on 200 trials for each contrast were analyzed according to temporal pattern. Threshold for discriminating a fine increment from a "basal" contrast slightly

above zero contrast was lower than for detecting a contrast against zero (Fig. 7A). Threshold then rose for higher basal contrasts to give a curve shaped like a "dipper" (6 of 7 cells; Fig. 7A). Increment threshold at the bottom of the dipper was lower than the detection threshold by 42% (Fig. 7A; $P \ll 0.01$; $t = 4.21$; df = 5; 1-tailed *t*-test). Basal contrast at the bottom of the dipper roughly matched the detection threshold (Fig. 7A, open vs. filled arrow) and also the sharp upturn of the contrast response function (arrow in Fig. 7B).

DISCUSSION

Alternative measures of contrast threshold

Ganglion cell contrast threshold in the intact anesthetized animal has been measured as the contrast that changes the spontaneous spike discharge over an extended interval by a criterion value, e.g., 2 SD (Barlow and Levick 1969; Derrington and Lennie 1982). This method is not optimal because it measures the average rate over a single bin and ignores variation of S/N ratio during the response. Thus if the S/N ratio
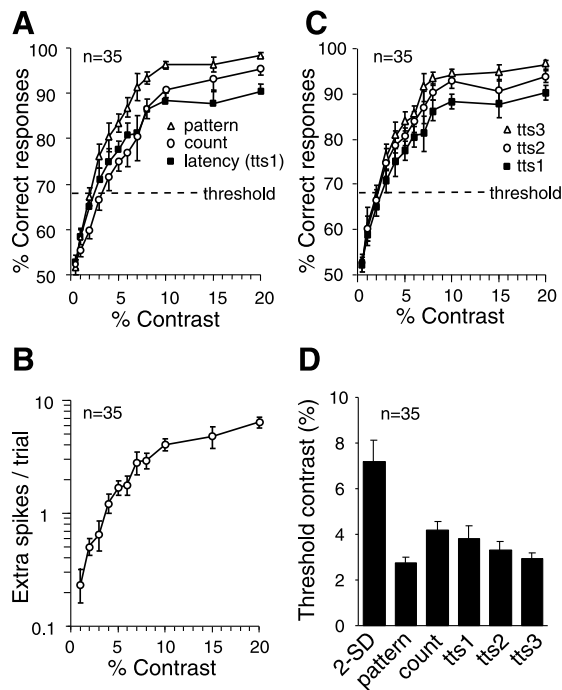
FIG. 6. Detection using different features of the spike train. *A*: performance with pattern, count, or latency (mean ± SE). Pattern performed best at all contrasts; latency performed better than count at lower contrasts but worse at higher contrasts. *B*: extra spikes per trial above maintained rate (mean ± SE). A near-threshold contrast (3–4%) evoked on average 1 extra spike, whereas higher contrasts evoked multiple spikes. *C*: when times to 2nd (tts2) or 2nd and 3rd (tts3) spikes were included, performance improved, mainly at higher contrasts (mean ± SE). *D*: detection threshold measured with different methods (mean ± SE). Pattern gave the lowest mean threshold.

varies, this method omits some of the available information. Furthermore, it fixes the error rates (false negative = 50% and false positive = 0.2–2%) and thus does not minimize their sum.

The IO method circumvents these problems (Geisler et al. 1991). It compares the noise distributions in the response to select the stimulus that most likely evoked a response. This method, rather than fixing the positive and negative error rates, minimizes their sum. The IO method (with spike count) applied to our brisk-transient cells gave a higher false positive rate (5–15%) but a lower false negative rate (15–25%) at threshold. The average threshold was lower than the 2-SD method by 1.7-fold (Figs. 6*D* and 8*A*).

This difference might have been predicted because d' (discrimination index) for our two-alternative forced-choice procedure is approximately twofold lower than for the 2-SD method (see Appendix I and Table 2 of Swets 1964). However, this prediction had not been tested for the ganglion cell spike train and would hold only if the probability distributions were normal. However, the spike distributions for some of our cells were not normal (Fig. 5). Thus the ratio of thresholds (2-SD method/IO spike count) varied across cells (Fig. 8*A*) and increased with the maintained rate (Fig. 8*B*).

The IO method using temporal pattern gave average thresholds that were 35% lower than the IO method using spike count. This advantage increased with maintained rate, reaching more than twofold at maintained rates of approximately 20 Hz (Fig. 8*B*). The reason is that a cell with a high maintained rate

often responded biphasically, rising above the mean for 50–100 ms and dropping below the mean for a comparable period. The spike count analysis pools the two phases and thus loses some information. This could be overcome by analyzing only the positive phase (Barlow and Levick 1969) but that would discard information in the negative phase. The temporal pattern analysis divides the entire trial period into small time bins and effectively weighs each bin according to its information content, thus optimally using all the information. Optimal bin size, determined for each cell near threshold, varied from 30 to 50 ms. This temporal resolution for a spot stimulus at low contrast is relatively coarse compared with the millisecond resolution for a white noise stimulus at high contrast (Keat et al. 2001; Reinagel and Reid 2000).
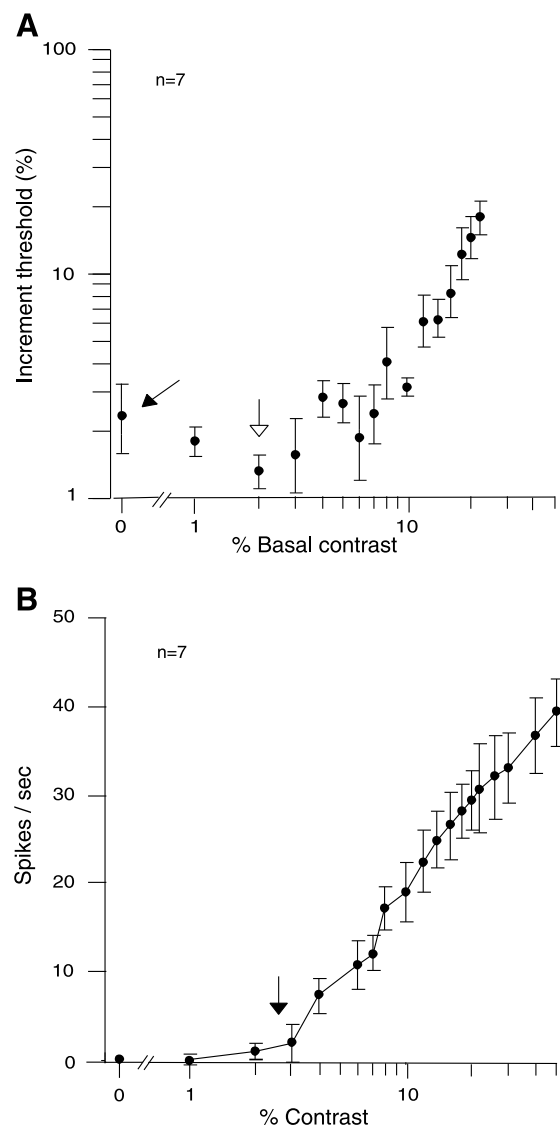

FIG. 7. Contrast discrimination is better than detection. *A*: discrimination between 2 fine contrasts was more sensitive than detection of a low contrast against the mean background. Discrimination threshold at a basal contrast of 2% (empty arrow) was 42% lower than detection threshold at a basal contrast of 0% (filled arrow). *B*: contrast response function of the cells shown in *A*. Spike responses (mean ± SE) are normalized for the maintained rate. Arrow marks the mean detection threshold for these cells. Responses to subthreshold contrasts were nearly 0. This might explain the "dipper-shaped" curve in *A*.
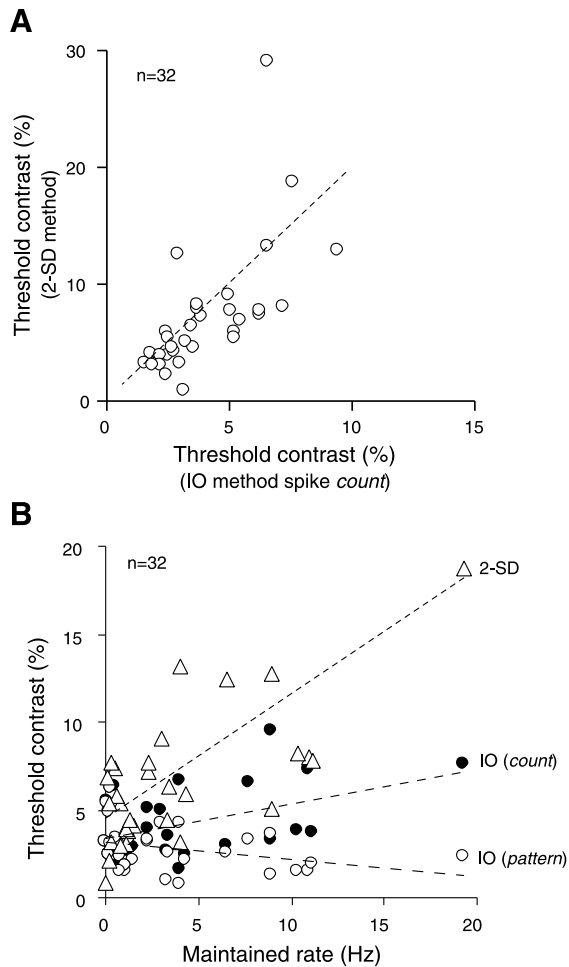
FIG. 8. Comparison of thresholds with IO and 2-SD method. *A*: dashed line represents the ratio of thresholds for the 2-SD and IO (count) methods predicted by the difference in their discrimination indexes (d′). The data points for most of our cells lie below the dashed line (average ratio = 1.7 ± 0.8 SD; $R^2 = 0.41$). *B*: threshold by IO (pattern) was relatively insensitive to maintained rate, but thresholds by IO (count) and 2-SD methods rose with maintained rate. Dashed lines are linear fits.

Ganglion cell sensitivity in vitro

Many studies are now performed on mammalian retina maintained in vitro (e.g., Ames and Nesbett 1981; Brown and Masland 2001; Chichilnisky and Kalmar 2002; Demb et al. 2001; DeVries and Baylor 1997; Freed 2000; Smith et al. 2001), but it is not known how well sensitivity in these circuits is preserved. Furthermore, in vitro studies are conducted at various temperatures, from "room temperature" to 37°C, but it is not known how temperature affects circuit performance. Temperature might affect a complex circuit more than would be predicted from the effect on basal metabolism or membrane current. Here we show for the in vitro retina attached to the pigment epithelium that a ganglion cell responds to bright stimuli that drive cone circuits for several hours without decrement of sensitivity (Fig. 2*C*). Raising the temperature from 25°C to 37°C lowered the contrast threshold by 2.5-fold (Fig. 3*B*). The effects on signal and noise were equal, and the net effect ($Q_{10} = 2.11$) was nearly identical to that for metabolism and membrane currents (Ames et al. 1992; Baylor et al. 1983; Lamb 1984) with no added factor for "complexity." This

measurement provides some basis for temperature corrections in future in vitro studies.

Detection versus discrimination

With the IO method using temporal pattern ganglion cell detects an optimal spot from background at contrasts as low as 0.8% (Fig. 5*E*). However, it discriminates an increment from a low basal contrast with even greater sensitivity (Fig. 7*A*). Discrimination threshold at a low basal contrast is more than 40% lower than detection threshold apparently because very low contrasts evoke hardly any response, and thus the gain (ΔResponse/ΔContrast) is lower (Fig. 7*B*; see also Chichilnisky and Kalmar 2002; Kim and Rieke 2001).

Cortical neurons also discriminate contrast increments more sensitively than they detect a low contrast against the mean background. Their "dip" in the increment threshold curve resembles that for the brisk-transient ganglion cells (approximately 40–50% below detection threshold; cf. Fig. 7*A* vs. Barlow et al. 1987 and Geisler et al. 1991). Plausibly therefore the ganglion cell dip might cause the cortical cell dip. In other words, the cortical cell's contrast threshold, both for detection and discrimination, might be limited by the ganglion cell. Finally, the psychophysical increment threshold curve also shows a similar dip, although slightly larger (approximately 70% below detection threshold; Banks et al. 1987; Nachmias and Kocher 1970; Nachmias and Sansbury 1974), and our results suggest that the ganglion cell dip might contribute to this.

Comparison to other species and psychophysics

Contrast thresholds of brisk-transient ganglion cells from the guinea pig visual streak in vitro can be reasonably compared with thresholds of brisk-transient/Y cells from the cat visual streak in vivo because the cells are similar in dendritic field size, cone convergence, membrane area, number of ribbon synapses, and input resistance (cat: Freed and Sterling 1988; Kier et al. 1995; O'Brien et al. 2002; guinea pig: M. A. Freed, Y.-H. Kao, L. Lassova, and P. Sterling, personal communication). For similar retinal illuminance and method of measurement (2-SD method) thresholds for the best ganglion cells in guinea pig were similar to those in cat and monkey, approximately 1% contrast (Fig. 5*E*) (Derrington and Lennie 1982, 1984; Linsenmeier et al. 1982). These comparisons are unavoidably imperfect because of differences in sampling of the maintained rate, retinal eccentricity, and stimulus calibration. Nevertheless, contrast threshold for the brisk-transient ganglion cell seems well conserved across species.

Since the brisk-transient ganglion cell in primate retina is the most sensitive type (Kaplan and Shapley 1986; Lee et al. 1990, 1995), its response threshold might limit psychophysical threshold for detection and discrimination of a small spot. Here is the reasoning. A behavioral response to a small stimulus can be no better than the collective response of a subset of ganglion cells. Ganglion cell signals are combined by cortical circuitry to produce visual behavior, and those with the highest S/N ratio (i.e., with the lowest thresholds) should dominate the summation (Pelli 1985). Ganglion cell signals with a smaller contribution from the stimulus would also contribute to psychophysical performance, but only to a limited extent, since with

similar noise (Croner et al. 1993) they would have a lower S/N ratio.

Psychophysical threshold for detecting a tiny square that would just fill the dendritic field of one brisk-transient cell (M cell) in human fovea at photopic levels is about 3% (Watanabe and Rodieck 1989; Watson et al. 1983). This stimulus would affect mainly one cell of this type because the dendritic fields "tile" with little overlap (Dacey and Brace 1992). Although about 25 brisk-sustained (P/midget) cells are cospatial with one M cell, the P cell is sixfold less sensitive and the optimal spot for the M cell covers the surrounds of all the P cells (Kaplan and Shapley 1986; Lee et al. 1990, 1995). Therefore at M cell threshold, P cells are unlikely to respond and thus will not contribute to the psychophysical detection. This would imply that psychophysical sensitivity to this spot is set mostly by one ganglion cell. If the human brisk-transient cell is as sensitive as the guinea pig brisk-transient ganglion cell (approximately 3%), which it may be, despite its smaller size (Croner and Kaplan 1995), this would imply very reliable transmission of the contrast signal across many levels of noisy synapses.

To this intriguing conclusion there are, of course, some objections: *1*) human brisk-transient cells might differ from guinea pig and *2*) additional brisk-transient ganglion cells might contribute to the psychophysical task. Regarding *1*), recall that the thresholds measured here resemble those measured in several other species including primate and therefore may be near the mark. Regarding *2*), the present approach can test the joint sensitivity of multiple spatial bins (to represent multiple cells) and thus can evaluate the contributions of additional brisk-transient cells, of both the same and complementary response polarity, so this proposition can be tested.

REFERENCES

Ames A and Nesbett FB. In vitro retina as an experimental model of the central nervous system. *J Neurochem* 37: 867–877, 1981.

Ames A, Li YY, Heher EC, and Kimble CR. Energy metabolism of rabbit retina as related to function: high cost of Na$^+$ transport. *J Neurosci* 12: 840–853, 1992.

Banks MS, Geisler WS, and Bennet PJ. The physical limits of grating visibility. *Vision Res* 27: 1915–1924, 1987.

Barlow HB. The Ferrier Lecture: the limiting factors in the design of the eye and visual cortex. *Proc R Soc Lond B Biol Sci* 212: 1–34, 1981.

Barlow HB, Kaushal TP, Hawken M, and Parker AJ. Human contrast discrimination and the threshold of cortical neurons. *J Opt Soc Am A* 4: 2366–2371, 1987.

Barlow HB and Levick WR. Three factors limiting the reliable detection of light by retinal ganglion cells of the cat. *J Physiol* 200: 1–24, 1969.

Baylor DA, Matthews G, and Yau KW. Temperature effects on the membrane current of retinal rods of the toad. *J Physiol* 337: 723–734, 1983.

Boycott BB and Wassle H. The morphological types of ganglion cells of the domestic cat's retina. *J Physiol* 240: 397–419, 1974.

Brainard DH. The psychophysics toolbox. *Spat Vis* 10: 433–436, 1997.

Brown SP and Masland RH. Spatial scale and cellular substrate of contrast adaptation by retinal ganglion cells. *Nature Neurosci* 4: 44–51, 2001.

Chander D and Chichilnisky EJ. Adaptation to temporal contrast in primate and salamander retina. *J Neurosci* 21: 9904–9916, 2001.

Chichilnisky EJ and Kalmar RS. Functional asymmetries in ON and OFF ganglion cells of primate retina. *J Neurosci* 22: 2737–2747, 2002.

Cleland BG, Levick WR, and Sanderson KJ. Properties of sustained and transient ganglion cells in the cat retina. *J Physiol* 228: 649–680, 1973.

Croner LJ and Kaplan E. Receptive fields of P and M ganglion cells across the primate retina. *Vision Res* 35: 7–24, 1995.

Croner LJ, Purpura AK, and Kaplan E. Response variability in retinal ganglion cells of primates. *Proc Natl Acad Sci USA* 90: 8128–8130, 1993.

Dacey DM and Brace S. A coupled network for parasol but not midget ganglion cells in the primate retina. *Vis Neurosci* 9: 279–290, 1992.

Davila KD and Geisler WS. The relative contribution of pre-neural and neural factors to areal summation in the fovea. *Vision Res* 31: 1369–1380, 1991.

Demb JB, Haarsma L, Freed MA, and Sterling P. Functional circuitry of the retinal ganglion cell's nonlinear receptive field. *J Neurosci* 19: 9756–9767, 1999.

Demb JB, Zaghloul K, Haarsma L, and Sterling P. Bipolar cells contribute to nonlinear spatial summation in the brisk-transient (Y) ganglion cell in mammalian retina. *J Neurosci* 21: 7447–7454, 2001.

Derrington AM and Lennie P. The influence of temporal frequency and adaptation level on receptive field organization of retinal ganglion cells in cat. *J Physiol* 333: 343–366, 1982.

Derrington AM and Lennie P. Spatial and temporal contrast sensitivities of neurones in lateral geniculate neucleus of macaque. *J Physiol* 357: 219–240, 1984.

DeVries SH and Baylor DA. Mosaic arrangement of ganglion cell receptive fields in rabbit retina. *J Neurophysiol* 78: 2048–2060, 1997.

Enroth-Cugell C and Robson J. The contrast sensitivity of retinal ganglion cells of the cat. *J Physiol* 187: 517–552, 1966.

Freed MA. Rate of quantal excitation to a retinal ganglion cell evoked by sensory input. *J Neurophysiol* 83: 2956–2966, 2000.

Freed MA and Sterling P. The ON-alpha ganglion cell of the cat retina and its presynaptic cell types. *J Neurosci* 8: 2303–2320, 1988.

Geisler WS, Albrecht DG, Salvi RJ, and Saunders SS. Discrimination performance of single neurons: rate and temporal-pattern information. *J Neurophysiol* 66: 334–362, 1991.

Green DM and Swets JA. *Signal Detection Theory and Psychophysics.* New York: Wiley, 1974.

Kaplan E and Shapley RM. The primate retina contains two types of ganglion cells, with high and low contrast sensitivity. *Proc Natl Acad Sci USA* 83: 2755–2757, 1986.

Keat J, Reinagel P, Reid RC, and Meister M. Predicting every spike: a model for the responses of visual neurons. *Neuron* 30: 803–817, 2001.

Kier CK, Buchsbaum G, and Sterling P. How retinal microcircuits scale for ganglion cells of different size. *J Neurosci* 15: 7673–7683, 1995.

Kim KJ and Rieke F. Temporal contrast adaptation in the input and output signals of salamander retinal ganglion cells. *J Neurosci* 21: 287–299, 2001.

Lamb TD. Effects of temperature changes on toad rod photocurrents. *J Physiol* 346: 557–578, 1984.

Lee BB, Pokorny J, Smith VC, Martin PR, and Valberg A. Luminance and chromatic modulation sensitivity of macaque ganglion cells and human observers. *J Opt Soc Am A* 7: 2223–2236, 1990.

Lee BB, Wehrhahn C, Westheimer G, and Kremers J. The spatial precision of macaque ganglion cell responses in relation to vernier acuity of human observers. *Vision Res* 35: 2743–2758, 1995.

Linsenmeier RA, Frishman LJ, Jakiela HG, and Enroth-Cugell C. Receptive field properties of X and Y cells in the cat retina derived from contrast sensitivity measurements. *Vision Res* 22: 1173–1183, 1982.

Liu CT. Energy balance and growth rate of outbred and inbred male guinea pigs. *Am J Vet Res* 49: 1752–1756, 1988.

Meister M and Berry MJ. The neural code of the retina. *Neuron* 22: 435–450, 1999.

Nachmias J and Kocher E. Visual detection and discrimination of luminance increments. *J Opt Soc Am* 60: 382–389, 1970.

Nachmias J and Sansbury RV. Grating contrast: discrimination may be better than detection. *Vision Res* 14: 1039–1042, 1974.

O'Brien BJ, Isayama T, Richardson R, and Berson DM. Intrinsic physiological properties of cat retinal ganglion cells. *J Physiol* 538: 787–802, 2002.

Peichl L, Ott H, and Boycott BB. Alpha ganglion cells in mammalian retinae. *Proc R Soc Lond B Biol Sci* 231: 169–197, 1987.

Pelli DG. Uncertainty explains many aspects of visual contrast detection and discrimination. *J Opt Soc Am A* 2: 1508–1532, 1985.

Pelli DG. The Video Toolbox software for visual psychophysics: transforming numbers into movies. *Spat Vis* 10: 437–442, 1997.

Reinagel P and Reid RC. Temporal coding of visual information in the thalamus. *J Neurosci* 20: 5392–5400, 2000.

Rockhill RL, Daly FJ, MacNeil MA, Brown SP, and Masland RH. The diversity of ganglion cells in a mammalian retina. *J Neurosci* 22: 3831–3843, 2002.

Roska B and Werblin F. Vertical interactions across ten parallel, stacked representations in the mammalian retina. *Nature* 410: 583–587, 2001.

Smirnakis SM, Berry MJ, Warland DK, Bialek W, and Meister M. Adaptation of retinal processing to image contrast and spatial scale. *Nature* 386: 69–73, 1997.

Smith VS, Pokorny J, Lee BB, and Dacey DM. Primate horizontal cell dynamics: an analysis of sensitivity regulation in the outer retina. *J Neurophysiol* 85: 545–558, 2001.

Swets JA. *Signal Detection and Recognition by Human Observers: Contemporary Readings.* New York: Wiley, 1964.

Troy JB. Spatial contrast sensitivities of X and Y type neurons in the cat's dorsal lateral geniculate nucleus. *J Physiol* 344: 399–417, 1983.

Troy JB and Robson JG. Steady discharges of X and Y retinal ganglion cells of cat under photopic illuminance. *Vis Neurosci* 9: 535–553, 1992.

VanRullen R and Thorpe SJ. Surfing a spike wave down the ventral stream. *Vision Res* 42: 2593–2615, 2002.

Watanabe M and Rodieck RW. Parasol and midget ganglion cells of the primate retina. *J Comp Neurol* 289: 434–454, 1989.

Watson AB, Barlow HB, and Robson JG. What does the eye see best? *Nature* 302: 419–422, 1983.